Electronic Supplementary Material (ESI) for Journal of Materials Chemistry A.

Supporting information

An In-situ Solidifying Strategy Enabling High-voltage All-Solid-State Li-metal Batteries Operating at Room Temperature

Zhu Cheng,[a] Hui Pan,[a] Chao Li,[a] Xiaowei Mu,[a] Yueming Du,[a] Fan Zhang,[a] Xueping Zhang,[a] Ping He*[a] and Haoshen Zhou*[b]

[a] Center of Energy Storage Materials & Technology, College of Engineering and Applied Sciences, National Laboratory of Solid State Microstructures, Collaborative Innovation Center of Advanced Microstructures, Nanjing University.

E-mail: pinghe@nju.edu.cn; hszhou@nju.edu.cn;

[b] National Institute of Advanced Industrial Science and Technology (AIST), Umezono 1-1-1, Tsukuba, 305-8568, Japan. E-mail: hszhou@aist.go.jp

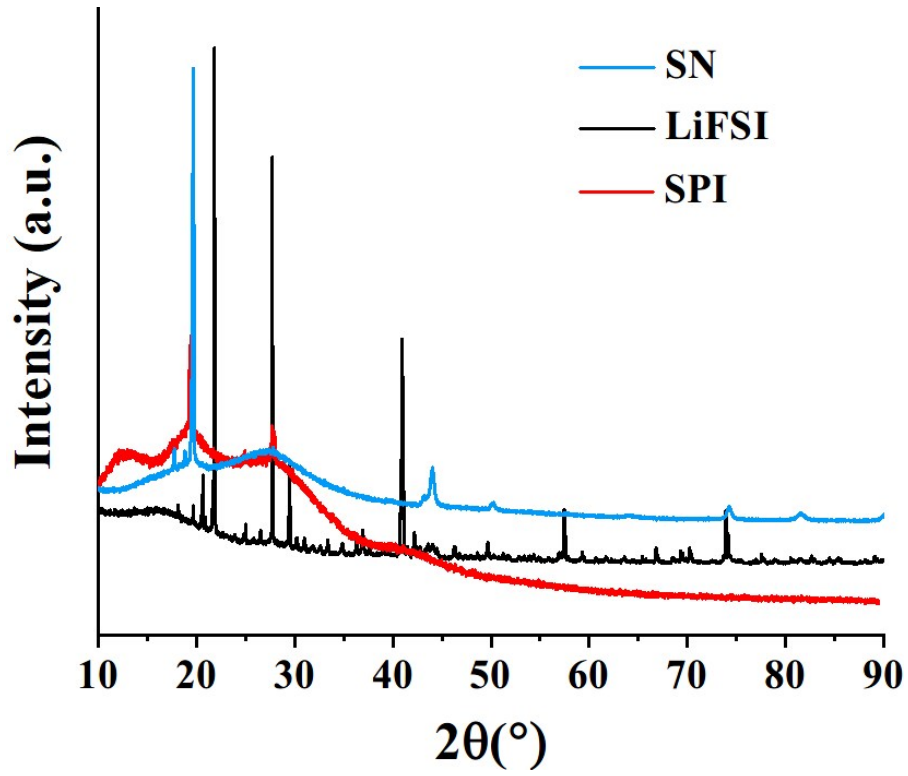

Figure S1. XRD pattern of SN,LiFSI and SPI.

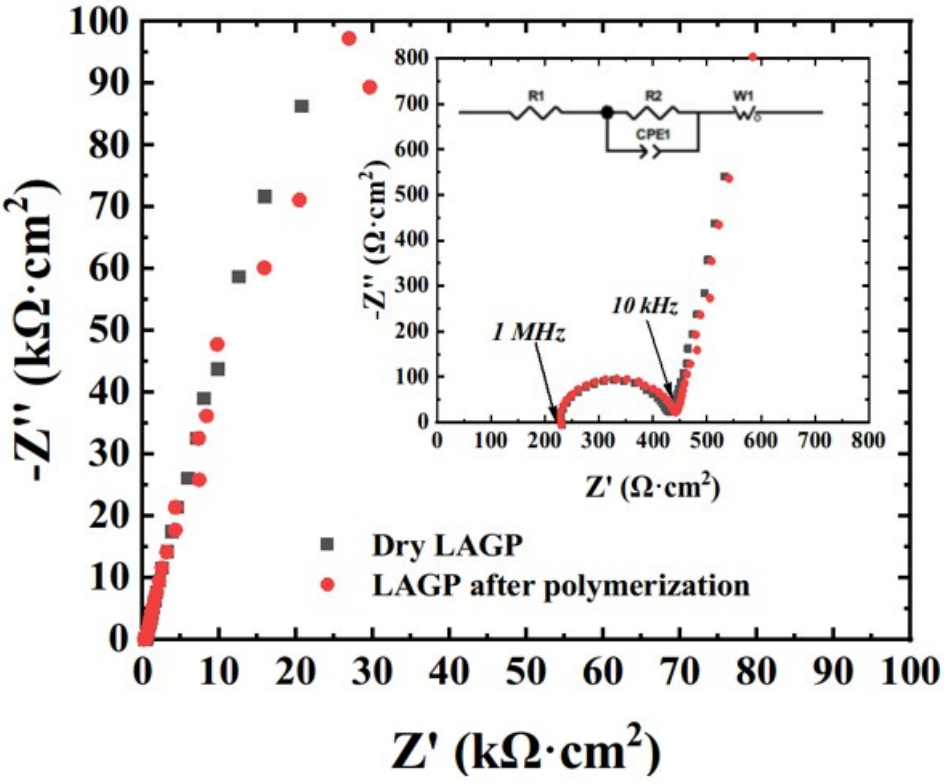

Figure S2. EIS result of LAGP with Au blocking electrodes. The frequency range is from 0.1 Hz to 1 MHz. The LAGP is ~600 μm thick and its diameter is ~16 mm.

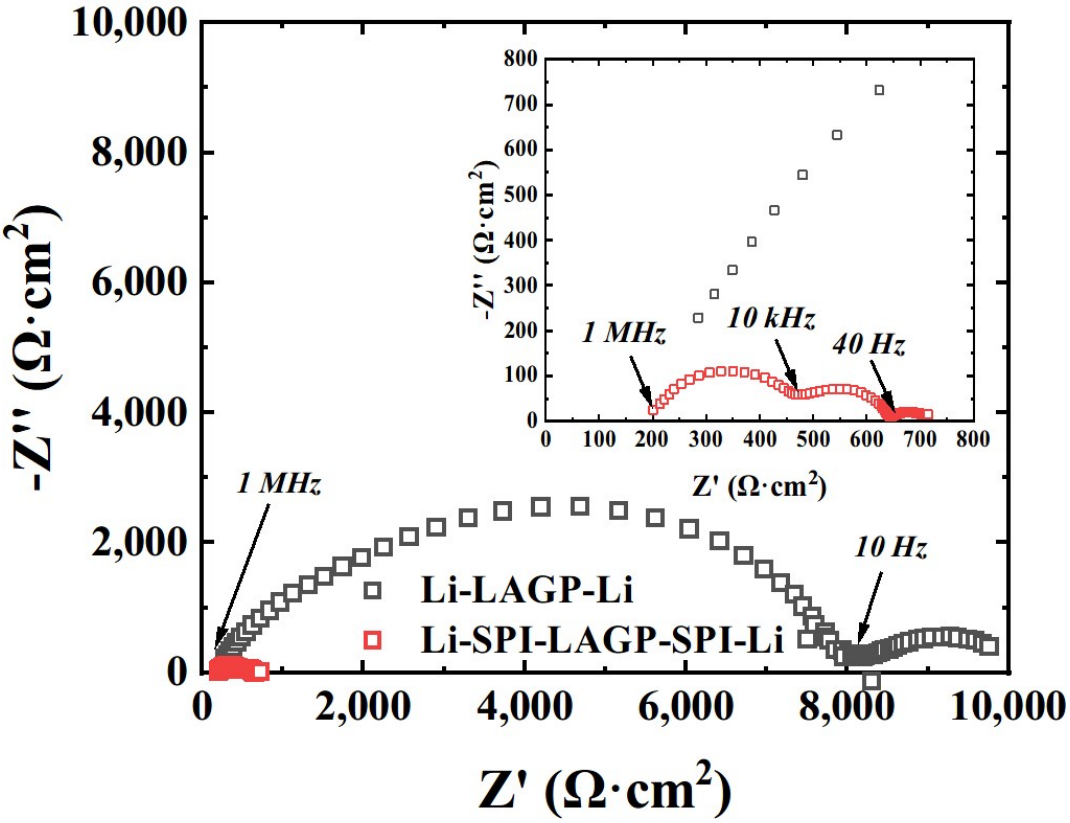

Figure S3. EIS result of the Li-LAGP-Li and Li-SPI-LAGP-SPI-Li symmetric cell.

Figure S4. The optical image of the LAGP pellet after cycling in Li-LAGP-Li cell.

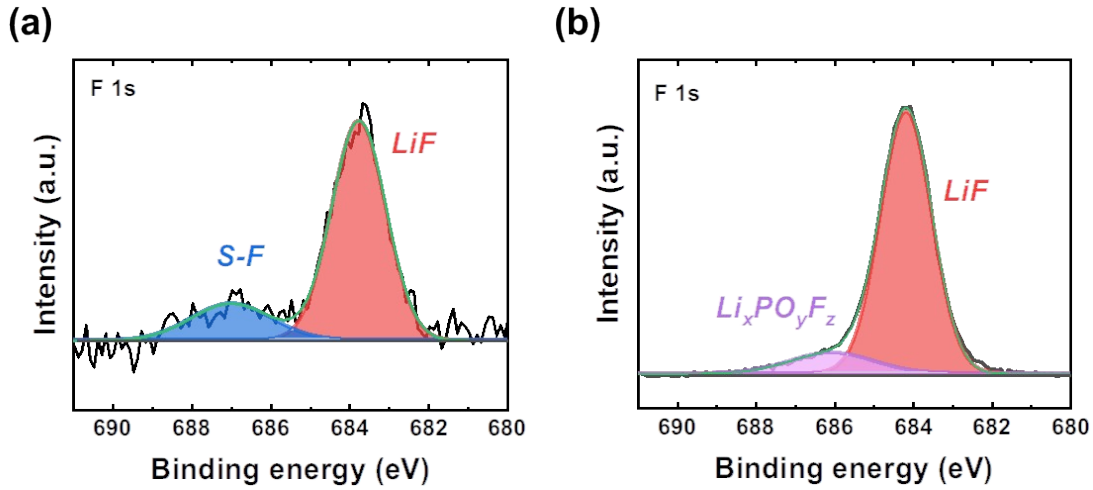

Figure S5. F 1s XPS results of the SEI in (a) Li-SPI-LAGP-SPI-Li cell and (b) Li-LE-LAGP-LE-Li cell.

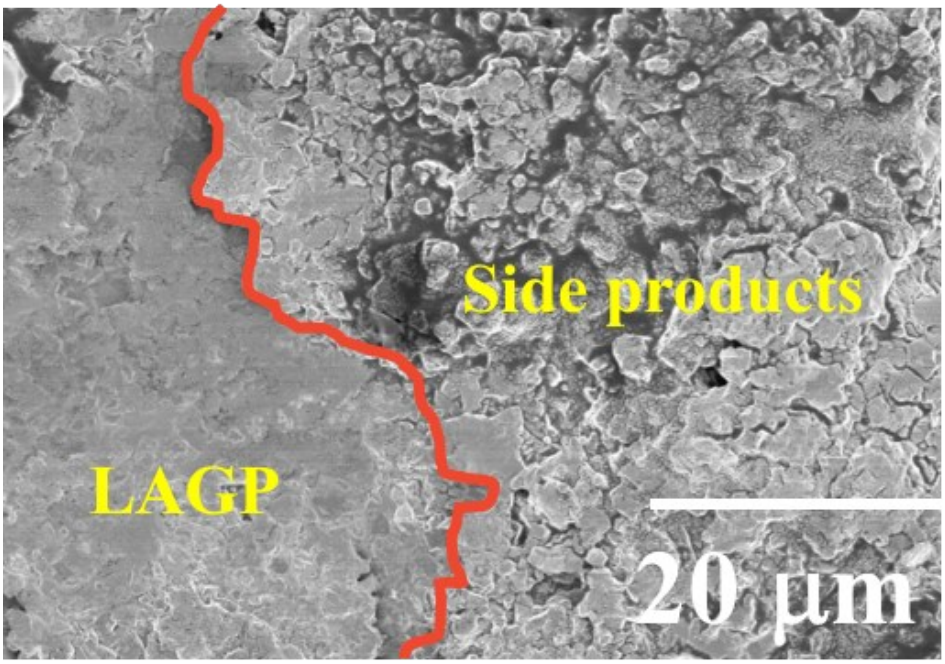

Figure S6. SEM image of the surface of LAGP pellet after cycling in Li-LE-LAGP-LE-Li symmetric cell.

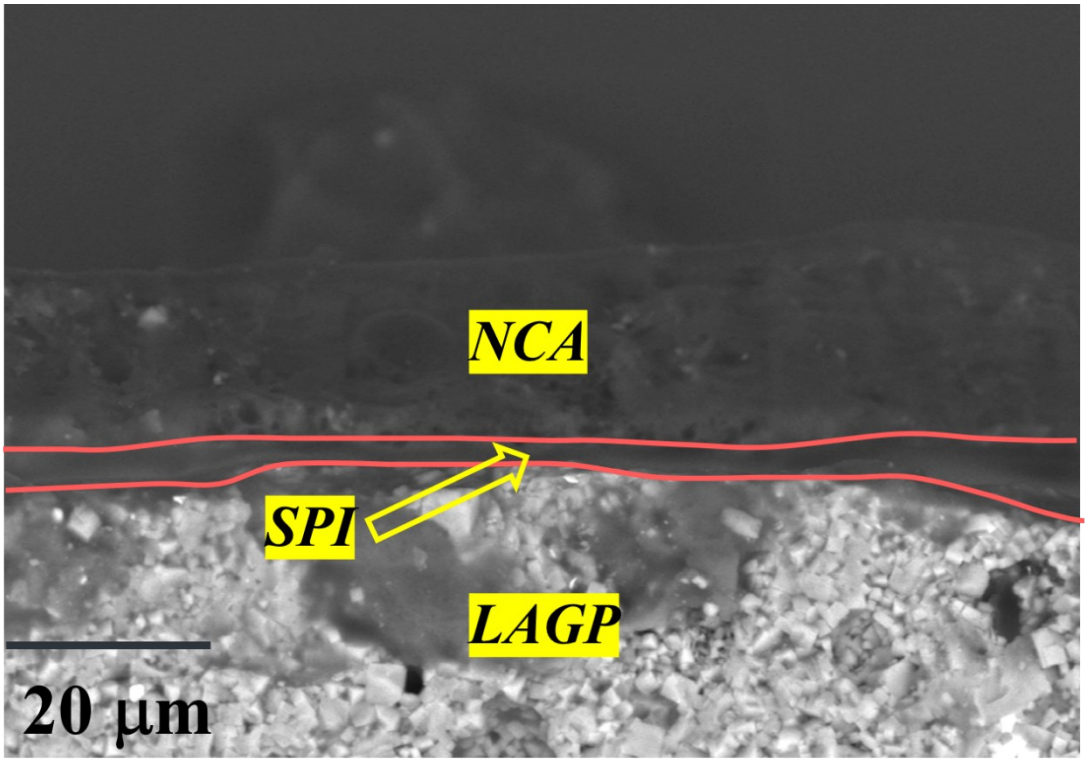

Figure S7. SEM image of the LAGP-NCA interface with SPI modification.

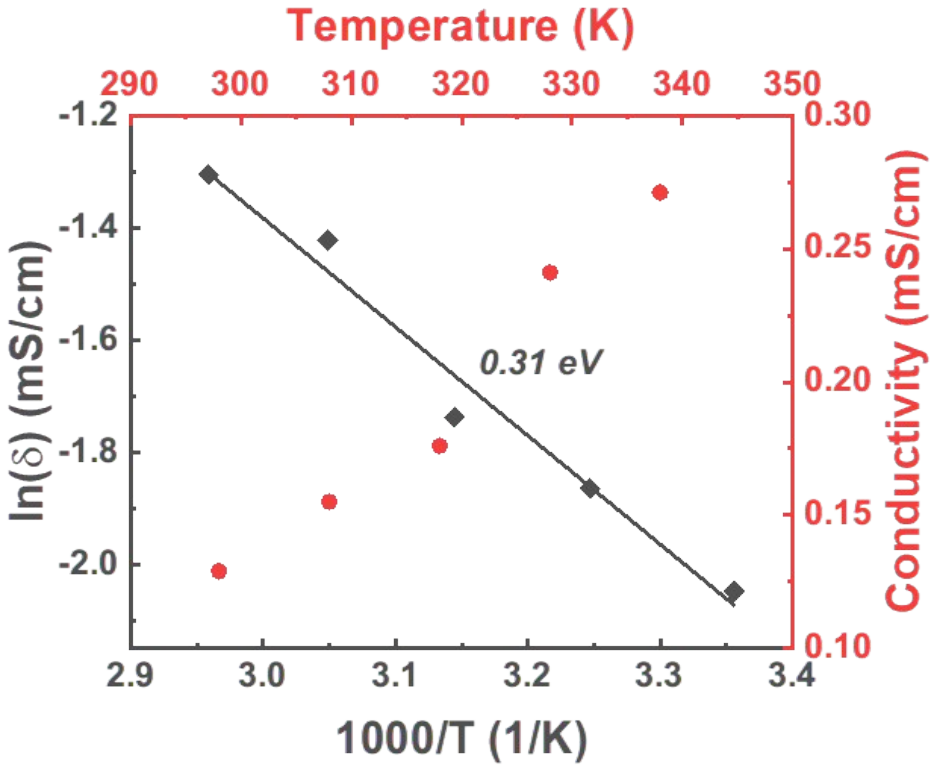

Figure S8. Temperature-dependent ionic conductivity of the LiTFSI-LiBOB based SPI

.

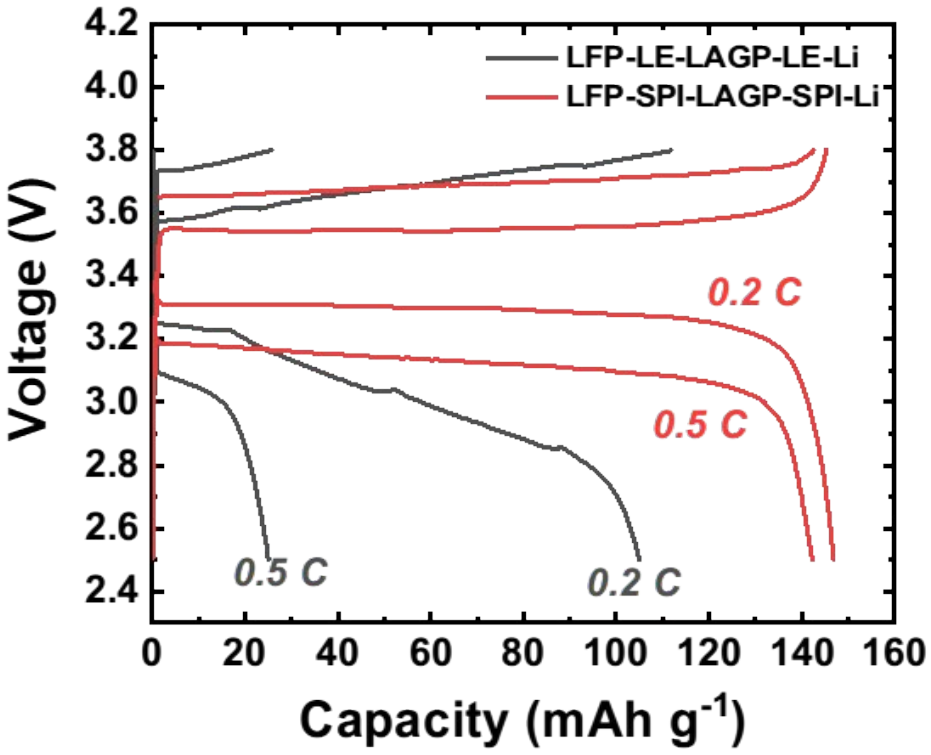

Figure S9. Voltage profile of the LFP-LE-LAGP-LE-Li and LFP-SPI-LAGP-SPI-Li cells at 0.2 C and 0.5 C.

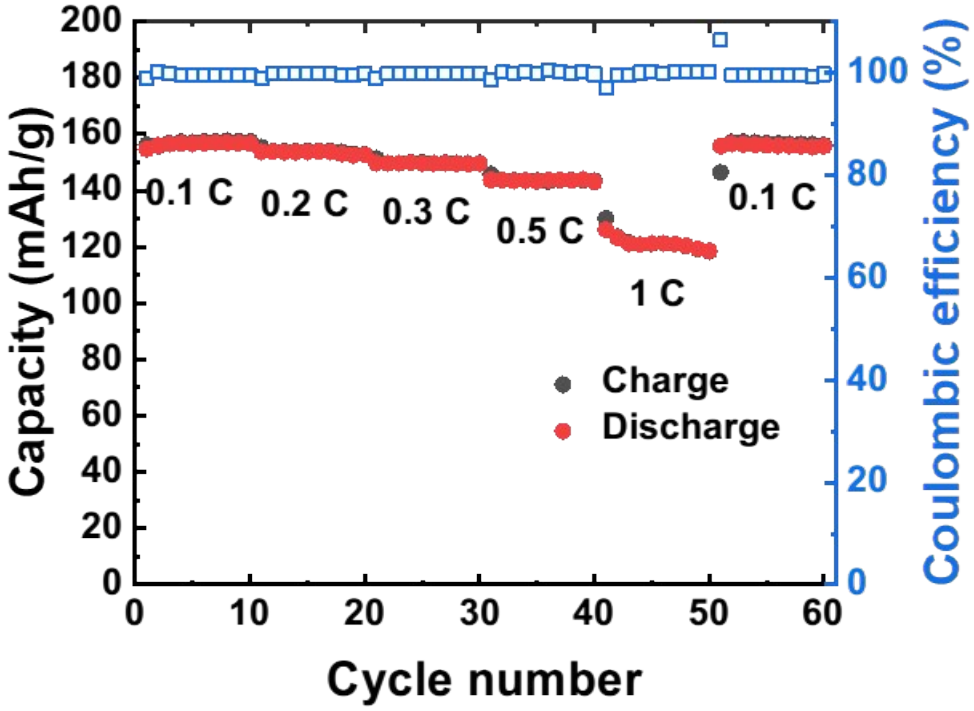

Figure 10. Rate performance of the LFP-SPI-LAGP-SPI-Li cell in the voltage range from 2.5 V to 3.8 V.

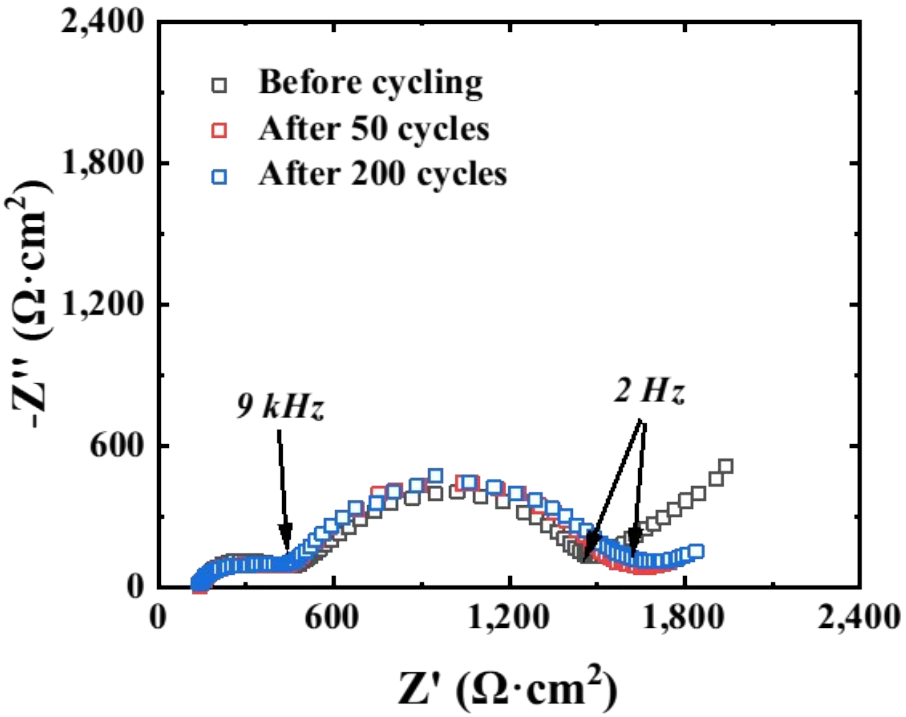

Figure S11. EIS result of the LFP-SPI-LAGP-SPI-Li cell before and after cycling.

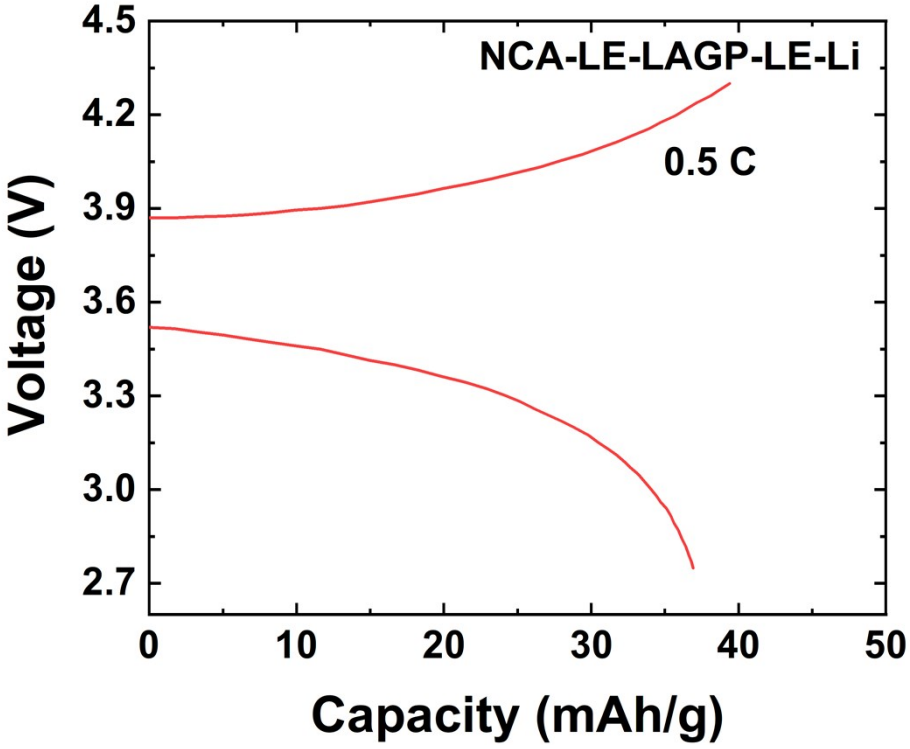

Figure S12. Voltage profile of NCA-LE-LAGP-LE-Li cell at 0.5 C.

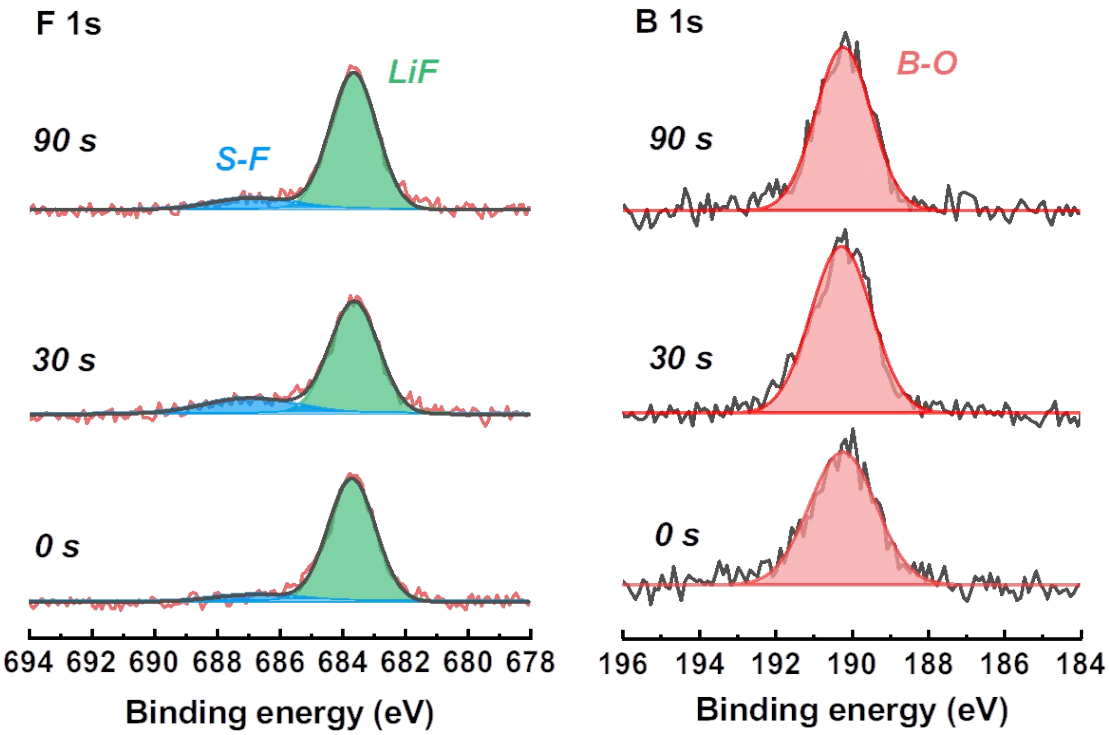

Figure S13. F 1s and B 1s XPS result of the CEI on cycled NCA cathode.

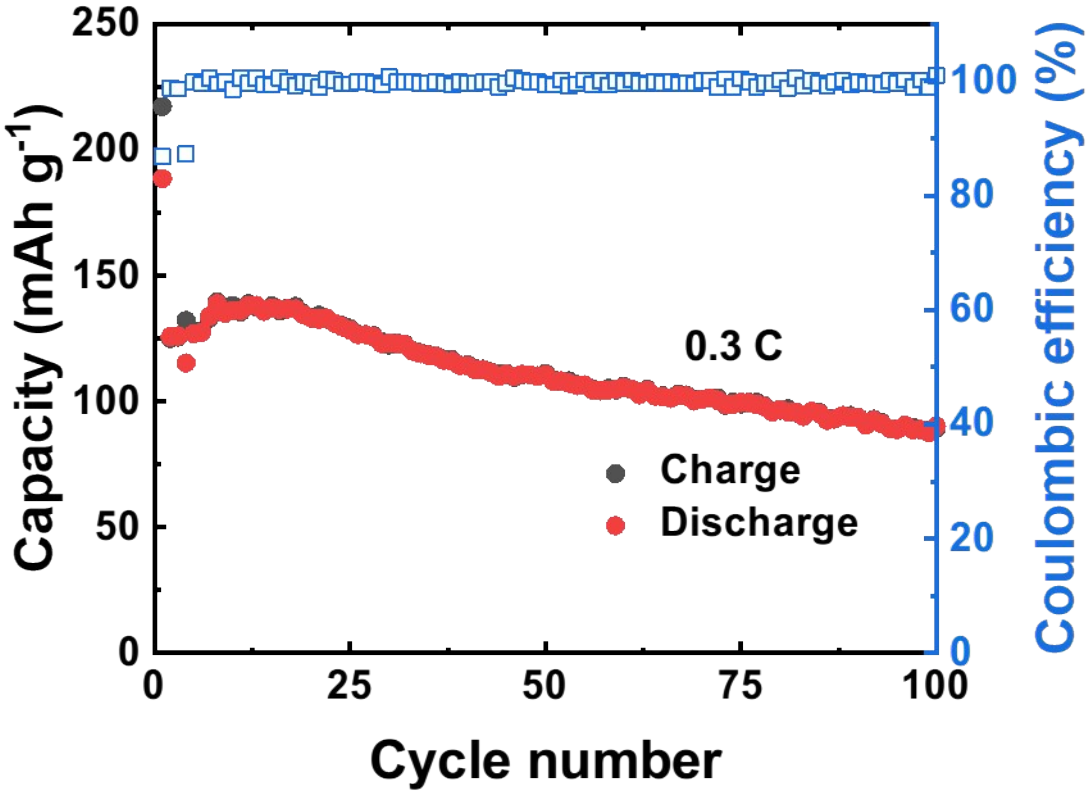

Figure S14. Cycling stability with Coulombic efficiency under 0.3 C for NCA-SPI-LAGP-SPI-Li cell in the voltage range from 2.75 V to 4.3 V.

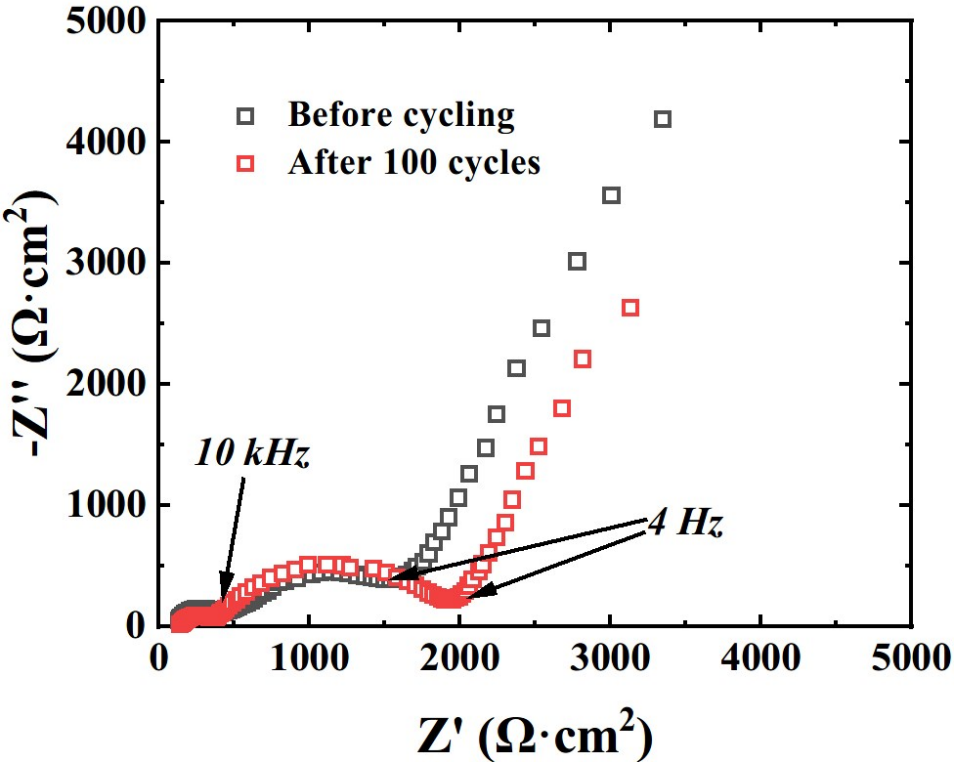

Figure S15. EIS result of the NCA-SPI-LAGP-NCA-Li cell before and after cycling.

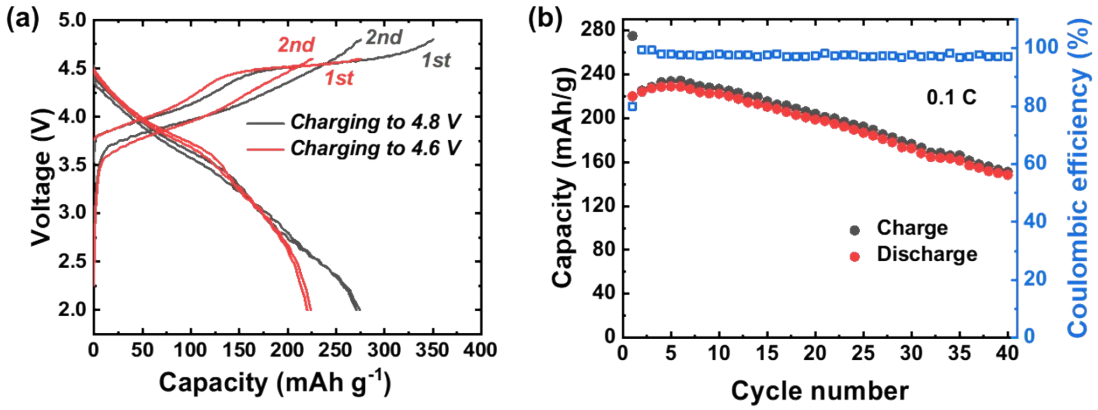

Figure S16. (a) Voltage profile of $Li_{1.2}Ni_{0.13}Co_{0.13}Mn_{0.54}O_2$-SPI-LAGP-SPI-Li cell for the first two cycles at 0.1 C in the voltage range from 2 V to 4.6 V and from 2 V to 4.8 V. (b) Cycling stability with Coulombic efficiency under 0.1 C for $Li_{1.2}Ni_{0.13}Co_{0.13}Mn_{0.54}O_2$-SPI-LAGP-SPI-Li cell in the voltage range from 2 V to 4.6 V.

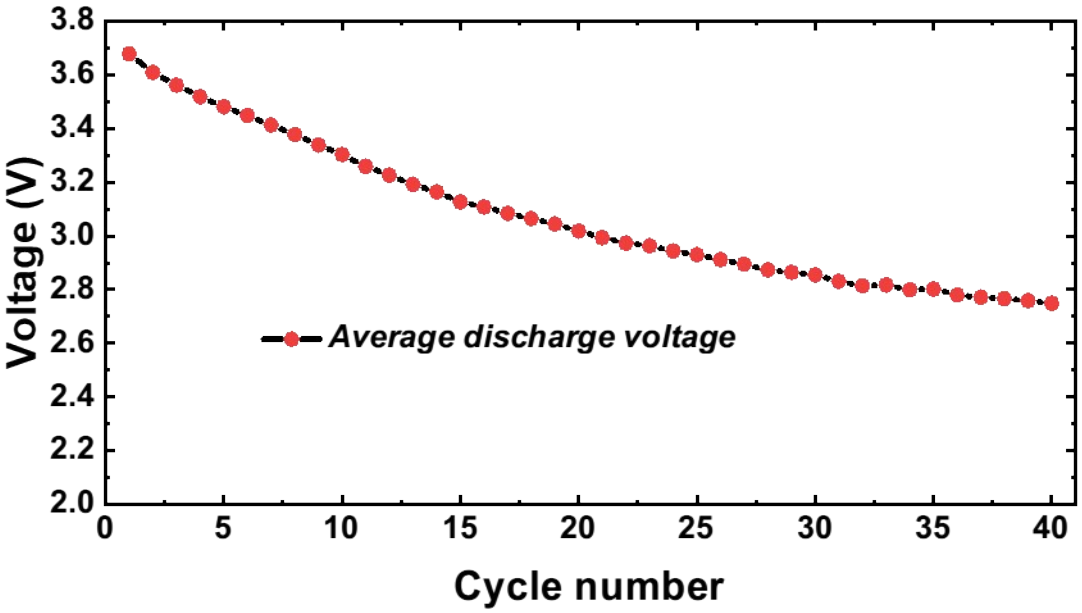

Figure S17. The evolution of average discharge voltage upon cycling for $Li_{1.2}Ni_{0.13}Co_{0.13}Mn_{0.54}O_2$-SPI-LAGP-SPI-Li cell at 0.1 C in the voltage range from 2 V to 4.6 V.

Table S1 Comparison of the CCD value achieved in this work and other reported oxide-electrolytes based symmetrical cells.

SSEs	Interfacial modification	Interfacial resistance (Ω cm^2)	CCD (mA cm^{-2})	Ref
$Li_7La_3Zr_2O_{12}$	None	5	0.6	1
$Li_{6.4}La_3Zr_{1.4}Ta_{0.6}O_{12}$	SnO_2	25	1.15	2
$Li_{1.5}Al_{0.5}Ge_{1.5}(PO_4)_3$	Bismuth layer	92.8	1.6	3
$Li_7La_3Zr_2O_{12}$	Cu_3N	83.4	1.5	4
$Li_{1.5}Al_{0.5}Ge_{1.5}(PO_4)_3$	Ionic liquid	5	>2	5
$Li_{1.5}Al_{0.5}Ge_{1.5}(PO_4)_3$	SPI	70	7	This work

References

1 A. Sharafi, C. G. Haslam, R. D. Kerns, J. Wolfenstine and J. Sakamoto, *J. Mater. Chem. A*, 2017, **5**, 21491–21504.

2 Y. Chen, M. He, N. Zhao, J. Fu, H. Huo, T. Zhang, Y. Li, F. Xu and X. Guo, *J. Power Sources*, 2019, **420**, 15–21.

3 F. Hu, Y. Li, Y. Wei, J. Yang, P. Hu, Z. Rao, X. Chen, L. Yuan and Z. Li, *ACS Appl. Mater. Interfaces*, 2020, **12**, 12793–12800.

4 H. Huo, Y. Chen, R. Li, N. Zhao, J. Luo, J. G. Pereira Da Silva, R. Mücke, P. Kaghazchi, X. Guo and X. Sun, *Energy Environ. Sci.*, 2020, **13**, 127–134.

5 S. Xiong, Y. Liu, P. Jankowski, Q. Liu, F. Nitze, K. Xie, J. Song and A. Matic, *Adv. Funct. Mater.*, , DOI:10.1002/adfm.202001444.